CHEMISTRY
A EUROPEAN JOURNAL

DOI: 10.1002/chem.201201061

Molecular Propellers that Consist of Dehydrobenzo[14]annulene Blades

Shunpei Nobusue,[a] Yuichi Mukai,[a] Yo Fukumoto,[a] Rui Umeda,[a, b] Kazukuni Tahara,[a] Motohiro Sonoda,[a, c] and Yoshito Tobe*[a]

Abstract: A new class of propeller-shaped compound (**4**), which consisted of dehydrobenzo[14]annulene ([14]DBA) blades, as well as its naphtho homologues (**5** and **6**), have been prepared. Although NMR studies of compound **4** did not provide useful information regarding its conformation in solution, DFT calculations with different functionals and the 6-31G* basis set all indicated that the D_3-symmetric structure was energetically more favorable than the C_2 conformer. From X-ray crystallographic analysis, it appeared that compound **4** adopted a propeller-shaped-, approximately D_3-symmetric structure in the solid state, in which the [14]DBA blades were twisted substantially owing to steric repulsion between the neighboring benzene rings. On the contrary, in the case of compound **6**, although the DFT calculations with the B3LYP functional predicted that the D_3-symmetric conformation was more stable, calculations with the M05 and M05-2X functionals indicated that the C_2 conformer was more favorable because of π–π interactions between the naphthalene units of a pair of neighboring blades. Indeed, X-ray analysis of compound **6** showed that it adopted an approximately C_2-symmetric conformation. Moreover, on the basis of variable-temperature ^{1}H NMR measurements, we found that compound **6** adopted a C_2 conformation and the barrier for interconversion between the C_2–C_2 conformers was estimated to be 16.2 kcal mol^{-1}; however, no indication of the presence of the D_3 isomer was obtained. The relatively small energy barriers to interconversion, despite the large overlapping of neighboring blades, was ascribed to the flexibility of the acetylene linkages, which could be deformed substantially in the transition state of the ring-flip.

Keywords: activation barrier · annulenes · density functional calculations · fused-ring systems · propeller-shaped compounds

Introduction

Propeller-shaped polycyclic aromatic compounds, which consist of a core benzene ring that is fused by three aromatic blades, have been attracting considerable interest in view of their unique conformations and their relevant dynamic behaviors.[1] These compounds include suitably substituted derivatives of triphenylene,[2] extended homologues of triphenylene, including hexabenzotriphenylene,[3–7] and decacyclenes,[8] which, in principle, can adopt C_2- and/or D_3 conformations. Pascal and co-workers reported that hexabenzotriphenylene (**1**), a prototypical propeller-shaped compound, adopted a strongly twisted D_3-symmetric conformation when it was synthesized by high-temperature vacuum pyrolysis of phenanthrene-9,10-dicarboxylic anhydride.[3] Through an extensive computational study, they concluded that the D_3 isomer of compound **1** was thermodynamically more stable than the C_2 isomer. They also proposed a rule of thumb for the C_2/D_3 dichotomy of sterically overcrowded triphenylene- and decacyclene derivatives: the D_3 conformation is preferred if the central benzene ring is expected to be aromatic (i.e., delocalized benzene-like bonds with a small degree of bond-alternation), whereas the C_2 conformation will be observed if the central ring is nonaromatic (i.e., bonds with a high degree of bond-alternation). In other words, this rule may be understood as follows: if the core benzene ring is less flexible (i.e., more resistant to deformation) than the blades, as in the case of compound **1**, the blades will be twisted into a chair-like form with D_3 symmetry, because such a twist will not disturb the overlap between the p orbitals in the peripheral aromatic rings. Conversely, if the blades are more resistant toward deformation than the core benzene ring, as in the case of substituted triphenylenes, the core benzene ring will be distorted into a twist boat-like form with C_2 symmetry because the local

---

[a] S. Nobusue, Y. Mukai, Y. Fukumoto, Dr. R. Umeda, Dr. K. Tahara, Dr. M. Sonoda, Prof. Y. Tobe
Division of Frontier Materials Science
Graduate School of Engineering Science, Osaka University
1-3 Machikaneyama, Toyonaka, Osaka 560-8531 (Japan)
Fax: (+81) 6-6850-6225
E-mail: tobe@chem.es.osaka-u.ac.jp

[b] Dr. R. Umeda
Current address:
Department of Chemistry and Materials Engineering
Faculty of Chemistry, Materials and Bioengineering
Kansai University, 3-3-35 Yamate, Suita, Osaka 564-8680 (Japan)

[c] Dr. M. Sonoda
Current address:
Department of Applied Chemistry
Graduate School of Engineering, Osaka Prefecture University
1-1 Gakuen-cho, Nakaku, Sakai, Osaka 599-8531 (Japan)

Supporting information for this article is available on the WWW under http://dx.doi.org/10.1002/chem.201201061; including general experimental methods.

overlap between the p orbitals of the peripheral benzene rings will be kept in this form. Pascal's rule was supported by several experimental observations. For example, Pérez, Guitián, and co-workers reported the isolation of the C_2 conformer of compound **1** as a kinetic product of the palladium-catalyzed cyclotrimerization of in-situ-generated 9,10-didehydrophananthrene and the conversion of the C_2 isomer into the D_3 isomer by heating.[4] The barriers ($\Delta G^{\neq}$) to the interconversion between the enantiomeric C_2 isomers and that of C_2–D_3 isomerization were determined to be 11.7 and 26.2 kcal mol^{-1}, respectively. The kinetically favored formation of the C_2 isomer was also observed in the nickel-catalyzed cyclotrimerization of 9,10-didehydrophenanthrene.[5] Very recently, the synthesis of the hexa-*tert*-butyl derivative of compound **1** by a regioselective $FeCl_3$-mediated Scholl cyclization was reported;[9] although its dynamic behavior was not described, it was shown to adopt a D_3-symmetric structure in the crystalline state by X-ray crystallography. In addition, Mount, Galow, and co-workers revealed that hexamethyltriphenylene (**2**), one of the ideal candidates for examining Pascal's C_2/D_3 dichotomy, underwent a rapid interconversion between two enantiomeric C_2 conformers and a slower C_2–D_3 interconversion, thus providing strong support for the rule.[2c]

We have previously reported the synthesis of the nominally D_{3h}-symmetric, triply fused dehydrobenzo[12]annulene (**3**), which consisted of 12-membered dehydroannulene rings.[10] DFT calculations predicted that it adopted an almost-planar conformation with a small twist angle of 7.5°, thus indicating that the steric crowding between the blades of compound **3** was small.[11] However, in the case of higher homologue **4** (Scheme 1), which contains dehydrobenzo[14]annulene rings,[12] and its naphthalene homologues (**5** and **6**), considerable overcrowding in the ground state is expected because it is not possible to draw a nominal D_{3h} structure without partial overlapping of the blades. This fact is more obvious in naphthalene homologues **5** and **6** than in compound **4** (for the structures of compounds **4**–**6** in the D_3- and C_2 conformations, optimized by DFT calculations, see the Supporting Information, Figure S1). Therefore, intuitively, the barriers to their conformational interconversion seem to be substantial, with those of compounds **5** and **6** being higher than that of compound **4**. If Pascal's rule is applicable to compounds **4**–**6**, they would be expected to adopt a D_3-symmetic conformation because the central ring must exhibit aromatic character (i.e., a small bond-length alternation) owing to the relatively weak aromaticity of the dehydrobenzo[14]annulene system. Because Pascal only argued about the choice of the C_2- and D_3 conformations for the triphenylene- and decacyclene-based propeller-shaped compounds, the structures of molecular propellers that contain blades with greater flexibility (owing to a large ring size as well as weak aromaticity) will provide information on how steric overcrowding affects the conformational selectivity.

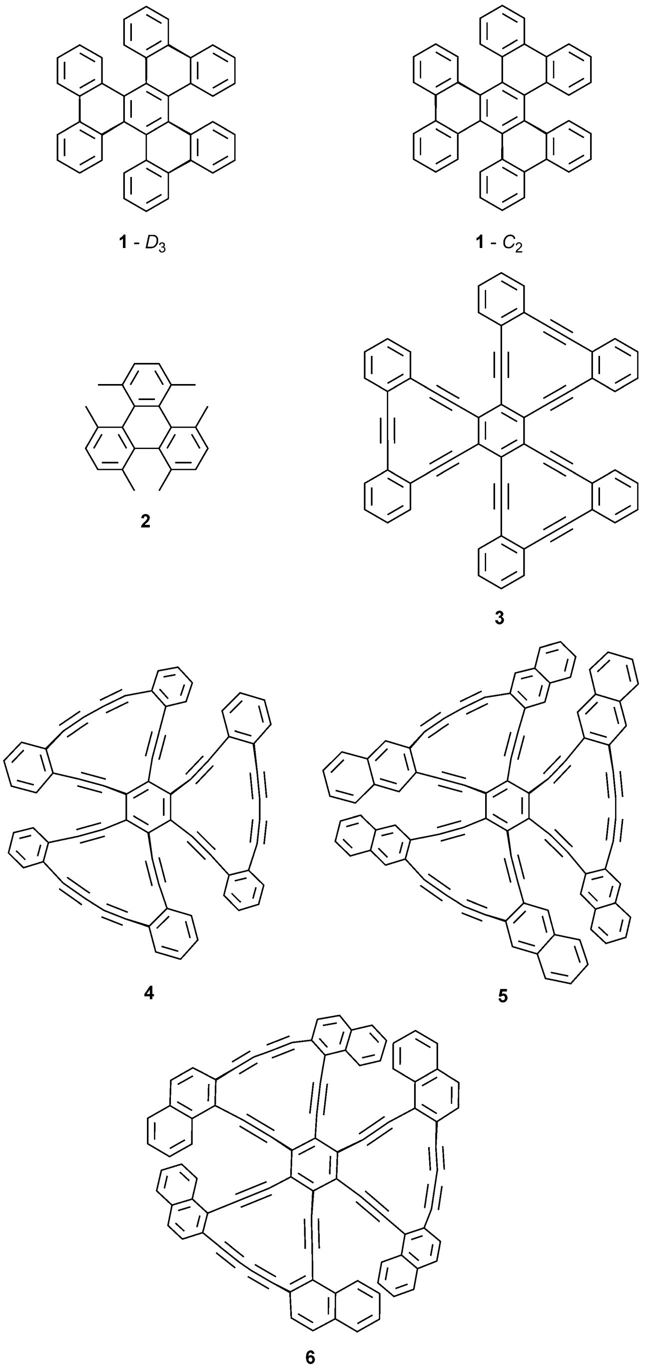

Scheme 1. Propeller-shaped polycyclic aromatic compounds, including target compounds **4**–**6**.

With regard to the conformational mobility of alkynes, it has been reported by Toyota and co-workers that a C−C≡C−C unit can be substantially deformed from linearity and that it behaves more flexibly than one may imagine in extremely overcrowded transition states of conformational isomerization, in which this unit causes major steric hindrance.[13] However, from the calculated geometries of the D_3-optimized structures (see the Supporting Information, Figure S1), the racemization of compounds **4**–**6** through ring-inversion of the [14]DBA blades seems to be difficult because the overlap with neighboring blades is so large that a heavily distorted transition state of the acetylene units is necessary for the slippage of the blades, although the conformational exchanges of compounds **1** and **2** took place with activation barriers that were smaller than one might imagine.[14] In this respect, it is interesting to see how flexible the [14]DBA blades are in the conformational interconversion of compounds **4**–**6**. Thus, we synthesized compounds **4**–**6** and investigated their conformational properties by using computational methods, X-ray crystallographic analysis, and variable-temperature NMR (VT-NMR) spectroscopy, the results of which are the topic of this article.

Results and Discussion

Synthesis of compounds 4–6: Compounds **4**–**6** were synthesized by attaching six diethynylarene units onto a central benzene ring, followed by intramolecular oxidative coupling, as shown in Scheme 2. For the preparation of compound **4** (Scheme 2a), the direct substitution of hexabromobenzene (**7**) with TMS-protected *o*-diethynylbenzene (**8**)[15] was carried out to give a six-fold-substitution product (**9**) in 37% yield. Removal of the TMS protecting group gave compound **10**, which was subjected without isolation to subsequent oxidative coupling by using Cu(OAc)$_2$·H$_2$O in pyridine at room temperature, thereby yielding compound **4** as a pale-yellow solid that quickly turned dark when the solvent was evaporated to dryness. The dark-brown solid was insoluble in any solvent. Because of its sensitivity, the exact yield of compound **4** in the final step was not determined.[16] Even in solution, the compound gradually darkened at room temperature. Only crystals that contained acetone (see below), which were used for the X-ray crystallographic analysis (Figure 2), could be stored without showing appreciable decomposition.

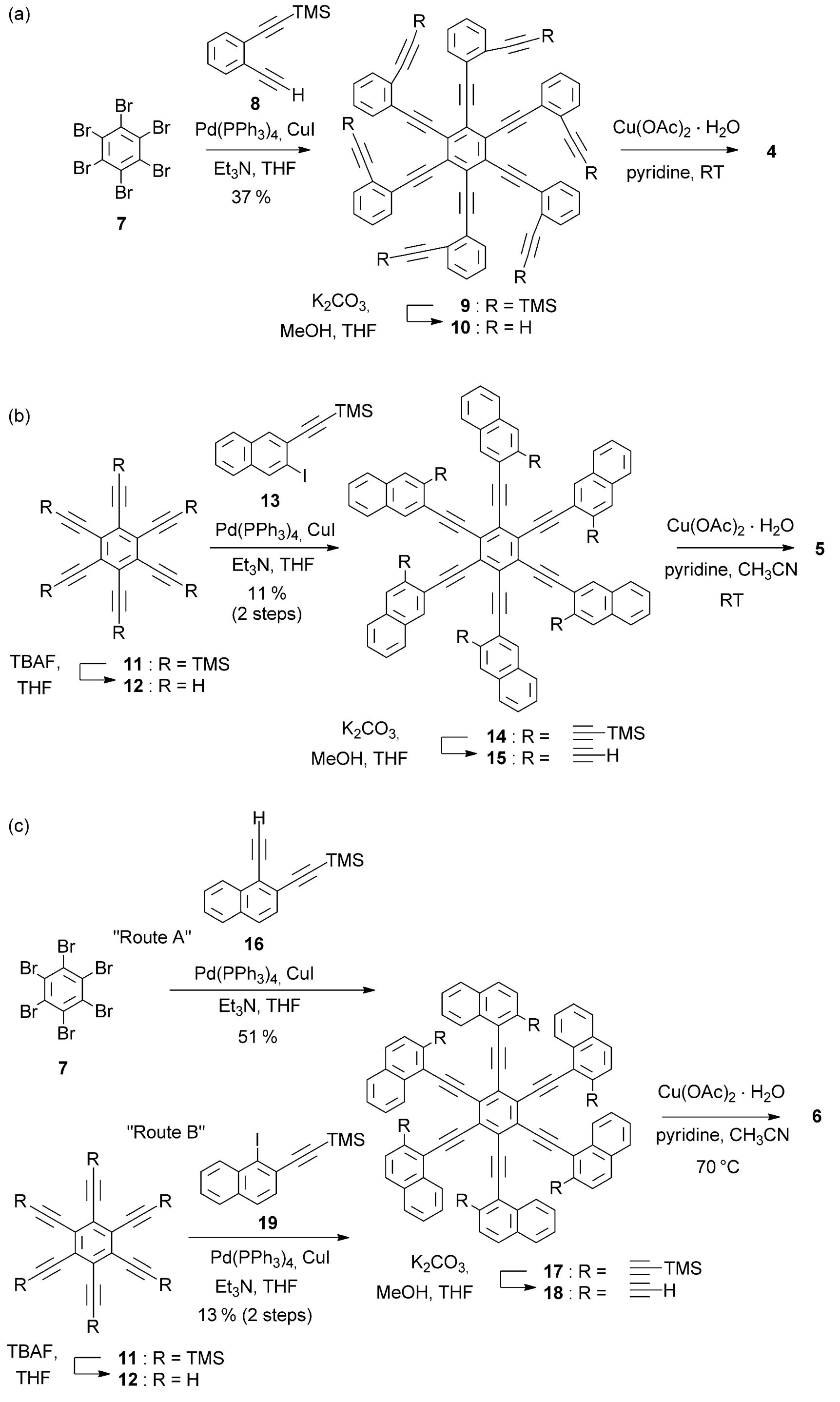

Scheme 2. Synthesis of compounds a) **4**, b) **5**, and c) **6**. TBAF = tetrabutylammonium fluoride, TMS = trimethylsilyl.

For the preparation of compound **5**, key precursor **14** was prepared by the cross-coupling of iodide **13** with hexaethynylbenzene (**12**)[17] because larger steric crowding may hinder the coupling reaction in a direct-substitution route (Scheme 2b). The Hagihara–Sonogashira coupling reaction of compound **12**, which was derived from its TMS derivative

(**11**),[18] with compound **13** gave six-fold-substitution product **14** in 11 % yield. After removal of the TMS group, oxidative coupling of compound **15** was conducted at room temperature in a similar manner to that of compound **10** to give naphthalene homologue **5** as a pale-yellow solid. Because compound **5** was even less stable than compound **4**, the yield was not determined exactly.

For the synthesis of compound **6**, the preparation of key precursor **17** was carried out through two pathways: "route A" and "route B" (Scheme 2c). As a result, whereas the cross-coupling of iodide **19** with hexaethynylbenzene (**12**) only gave compound **17** in 13 % yield (route B), the direct substitution of hexabromobenzene (**7**) with TMS-protected *o*-diethynylnaphthalene (**16**) gave compound **17** in up to 51 % yield (route A). The intramolecular oxidative coupling of compound **18**, which was derived from the removal of the TMS protecting group of compound **17**, was carried out at 70 °C, thereby yielding naphthalene homologue **6** in 7 % yield. Compound **6** was not obtained when the reaction was conducted at room temperature. Similar to compound **4**, compound **6** was only stable in crystals that contained solvent molecules. The absorption spectra of compounds **4**–**6**, as well as those of their key precursors (**9**, **14**, and **17**, respectively), are shown in the Supporting Information, Figure S2. Whilst compounds **9**, **14**, and **17** show broad absorption bands, compounds **4**–**6** exhibit absorptions with vibrational structures at longer wavelengths than their corresponding precursors.

Calculated relative stabilities of conformers of compounds 4–6: The interconversion between the C_2- and D_3-symmetric conformations of compound **4** is shown in Scheme 3; this interconversion represents one of the shortest possible pathways, assuming that the barrier for interconversion between two D_3 enantiomers through the synchronous inversion of three blades is too high. A full map for compound **6**, including all of conformational exchanges, is shown in the Supporting Information, Scheme S6. Apparently, interconversion between the D_3-symmetric enantiomers takes place through at least two C_2-symmetric diastereomers. To estimate the relative stabilities of the C_2- and D_3 conformers of compounds **4**–**6**, we performed semiempirical MO calculations (PM3) and DFT calculations at the B3LYP/6-31G*, M05/6-31G*, and M05-2X/6-31G* levels of theory. The relative energies are summarized in Table 1. Although the energy differences between the C_2- and D_3 conformations are smaller compared to compound **1**,[3] all of the computational results showed a preference for the D_3 conformation for compound **4**, in accord with Pascal's rule. On the other hand, the DFT calculations with the M05 series of functionals, which are known to adequately predict noncovalent interactions, such as π–π interactions,[19] tend to show a preference for the C_2 conformers; more specifically, the calculations with the M05-2X functional predicted that the C_2 conformer of 1,2-naphtho homologue **6** was significantly more stable than the D_3 conformer. The results from the M05/6-31G* calculations are always in-between these two extremes, thus favoring the D_3 form for compounds **4** and **5** and the C_2 form for compound **6**. The reason for the difference depending on the functional is discussed in the subsequent section, in comparison with their X-ray structures.

Table 1. Differences between the calculated energies for the D_3- and C_2 conformers of compounds **4**, **5**, and **6**.[a]

	PM3	DFT: B3LYP/6-31G*	DFT: M05/6-31G*	DFT: M05-2X/6-31G*
4	0.79	1.97	1.71	1.56
5	0.84	2.00	0.54	−0.26
6	2.44	4.44	−1.08	−3.24

[a] $\Delta H_f^\circ(C_2)-\Delta H_f^\circ(D_3)$ (PM3) and $E(C_2)-E(D_3)$ (DFT), in kcal mol^{-1}. Positive values indicate a preference for the D_3 conformation. The individual energy is given in the Supporting Information, Table S1.

Single-crystal- and theoretical structures of compounds 4 and 6: X-ray crystallographic analysis of compound **4** was carried out for crystals that contained a disordered acetone molecule because it was stabilized in the acetone-containing crystals. The parent [14]DBA was also reported to be unstable and even polymerize in crystals.[20] However, some arylbutadiyne derivatives, which are unstable in concentrated solutions and as amorphous solids, are known to become substantially more stable in crystals.[21]

The crystal contains a pair of *P*- and *M*-enantiomers that adopt an approximate D_3-symmetric conformation with a propeller-shape, thereby indicating the preference for this conformation in the crystalline state. The twisting of the three [14]DBA blades is not equal, most probably owing to the presence of a disordered acetone molecule that is locat-

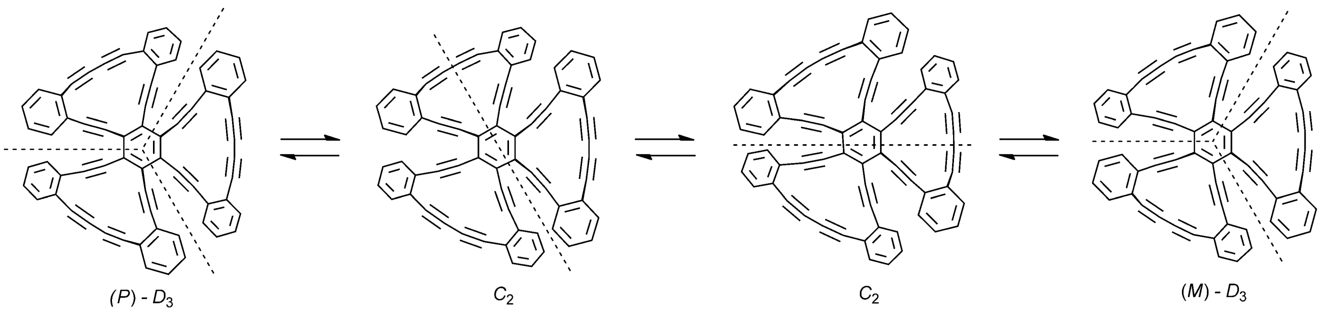

Scheme 3. One of the shortest pathways for interconversion between the D_3 isomers.

ed atop ring A (Figure 1). The nonbonded distances between the closest carbon atoms of the terminal benzene rings of adjacent blades (C18⋅⋅⋅C27, C40⋅⋅⋅C49, and C62⋅⋅⋅C5 are 3.414, 3.276, and 3.495 Å, respectively) indicate that the blade that is near the solvent molecule (ring A) is more distorted than the other two because of the steric conflict (atom labeling is shown in Figure 1). The averaged nonbonding distance is 3.395 Å, which is almost equal to the sum of the van der Waals radii of the carbon atoms. The dihedral angles between the central benzene ring and the three peripheral mean planes, C4−C19, C26−C41, and C48−C63, are relatively small (24.5°, 23.0°, and 29.3°, respectively) compared to those of compound **1** (28.2–30.0°), thus indicating that the distortion is shared by the triple bonds. The average bond length of the central ring of compound **4** that is involved in the [14]DBA ring (endocyclic) is 1.405 Å, whereas that of the exocyclic bond is 1.428 Å. The alternation in bond length is less pronounced than that in compound **1** (1.397 versus 1.434 Å). In addition, the central ring of compound **4** adopts a much-shallower chair conformation, with dihedral angles of 4.14–7.20°, than those of compound **1** (dihedral angles: 14.8–17.6°). All of these results indicate that compound **4** is less distorted than compound **1**. The most-deformed triple bonds are found at the "spoke" bonds, such as C1−C2−C3, with an average angle of 167.3°, although such deformation is typically observed for other [14]DBA derivatives.[20]

Table 2 lists representative structural parameters for the D_3 conformer of compound **4** that were obtained from X-ray analysis and from DFT calculations with different functionals. The corresponding parameters for the D_3 conformers of compounds **5** and **6** are listed in the Supporting Information, Table S2. As shown in Table 2, the theoretical results with the M05-2X/6-31G* functional agreed reasonably well with the X-ray structure of compound **4** with regard to the bond lengths and -angles and reproduced the experimental data slightly better than the B3LYP/6-31G* method. On the other hand, the former results underestimate the twisting of the blades relative to the core benzene ring and, therefore, overestimate the close contact between the adjacent blades compared to the experimental data. This trend is in accord with the fact that the M05 series of functionals reproduce the molecular structures, which include noncovalent interactions, better than the most-frequently used B3LYP method, although they tend to overestimate the attractive interactions.[19]

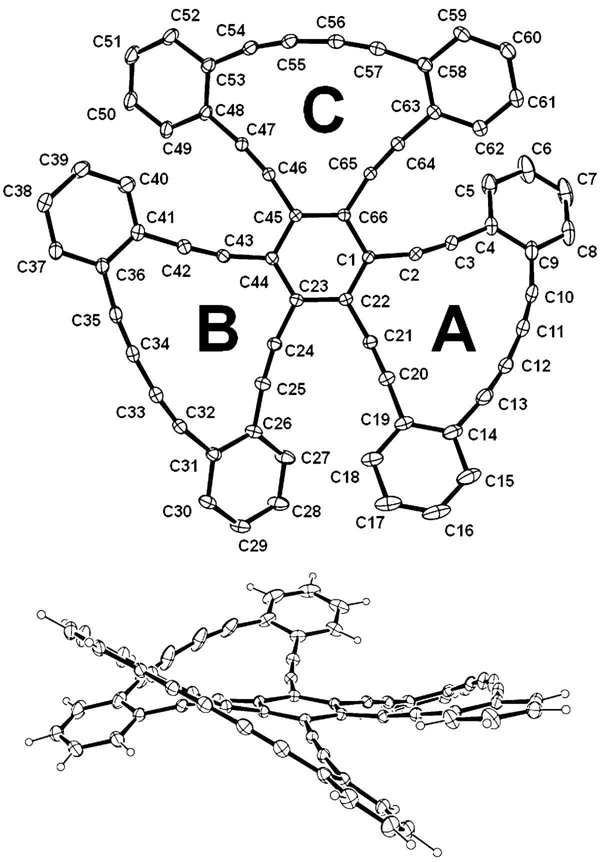

Figure 1. Molecular structure of compound **4** with atom-numbering, thermal ellipsoids at 30 % probability; solvent molecules are omitted for clarity (hydrogen atoms are omitted in the top structure for clarity).

Table 2. Comparison of the experimental- and calculated geometries of the D_3 isomer of compound **4**.

	X-ray[f]	B3LYP	M05	M05-2X
endocyclic bond length [Å][a]	1.405	1.416	1.412	1.405
exocyclic bond length [Å][b]	1.428	1.438	1.432	1.425
closest nonbonded distance [Å][c]	3.395	3.558	3.464	3.323
core–blade dihedral angle [°][d]	25.55	19.52	18.70	17.61
distorted triple-bond angle [°][e]	167.33	168.20	167.91	168.02

[a] Bond length of the central benzene ring that is endocyclic to the [14]DBA ring. [b] Bond length of the central benzene ring that is exocyclic to the [14]DBA ring. [c] Closest nonbonding distances between the closest carbon atoms of the terminal benzene rings of adjacent blades (i.e., C18⋅⋅⋅C27, Figure 1). [d] Dihedral angles between the mean plane of the central benzene ring and that of the diphenylbutadiyne unit (16 carbon atoms in total; i.e., C4−C19, Figure 1). [e] Bond angles around the "spoke" acetylene unit (e.g., C1−C2−C3, Figure 1). [f] For the experimental structure, the averaged values for the three- or six relevant distances/angles are given.

Crystals of compound **6** that were suitable for X-ray analysis were obtained by recrystallization from a mixture of *o*-dichlorobenzene and MeCN (Figure 2), although they contained two $C_6H_4Cl_2$ solvent molecules that were disordered atop- and below one of the distorted [14]DBA units (ring D). Similar to the case of compound **4**, compound **6** was stabilized in crystals that contained solvent molecules. Strikingly, in accord with the DFT calculations with the M05-2X functional, compound **6** adopted an approximately C_2-symmetric conformation in the crystalline state.

With regard to the bond-length alternations in the central ring, whereas the endocyclic bond lengths are 1.424 and 1.415 Å, the exocyclic bond lengths are 1.411 and 1.427 Å. That is, the bond lengths do not depend on whether the ring is endo- or exocyclic; two bonds (C1−C90 and C31−C60, Figure 2) are relatively short, whereas the other four bonds are relatively long. Therefore, the bond lengths of the central ring reflect the C_2 symmetry and do not exhibit alternating changes. Similar to the case of compound **4**, the bond-length difference is smaller than that of compound **1**.[3] Because compound **6** adopts a C_2-symmertic structure in spite of the aromatic character of the central ring, it may no longer be obliged to follow Pascal's rule.

The most-notable feature in the crystal structure of compound **6** is the unique structure of the two [14]DBA units, which are deformed into a "warped" shape. The third [14]DBA unit (ring E) adopts an almost-planar dinaphthylbutadiyne substructure. The bond angles of the acetylene "spoke" units (166.6–176.6°) are similar to those of compound **4**. However, the bond angles of the butadiyne units (165.0–168.7°) are slightly smaller than those of compound **4** (166.0–171.8°), although the similar degree of distortion has been frequently observed.[22] The dihedral angle between the naphthalene rings of the "warped" [14]DBA unit (i.e., C34–C43 versus C48–C57, Figure 2) is 39.8°.[23] To the best of our knowledge, the deformation of [14]DBAs in structures such as compound **6** has not been reported previously.

Another remarkable structural feature in the crystal structure of compound **6** is the small dihedral angles between the naphthalene rings in a pair of neighboring blades. That is, the two naphthalene units in blades D and F are almost parallel to each other, with a small dihedral angle of 6.1° between their mean planes. Moreover, the distances from each carbon atom of one naphthalene unit to the mean plane of the other naphthalene unit are in the range 3.185–3.553 Å, which is slightly shorter/longer than the sum of the van der Waals radii, thereby strongly indicating the presence of π–π stacking interactions. Such an overlapping geometry was not found in the naphthalene units between the D/E and E/F pairs, in which the dihedral angle was 37.4°.

The theoretical- and experimental (X-ray) structures of the C_2 conformer of compound **6** are compared in Table 3. Most of the structural parameters agree well, taking into account the presence of two *o*-dichlorobenzene molecules per molecule of compound **6** in the crystal. However, the most-notable difference was found between the theoretical structures, in particular in the relative geometry of the two closely located naphthalene rings. As described above, in the crystal structure, the naphthalene units in rings D and F were almost parallel to each other, with a small dihedral angle of 6.1° between the mean planes. This geometry was best reproduced in the calculations with the M05-2X functional, which showed a dihedral angle of 13.2°; the dihedral angles in the B3LYP and M05 structures were 29.9 and 17.3°, respectively. On the other hand, because the M05-2X functional tends to overestimate the noncovalent interactions, the dihedral angles between the naphthalene units in rings D/F and E/F are underestimated (15.4°) compared to the experimental result (37.4°). However, the overlapping geometry between the naphthalene rings of compound **6** suggests that π–π interaction may contribute to the stability of the C_2 conformer. To estimate the stabilization energy, single-point calculations were undertaken for two naphthalene molecules that were located at the same geometry as that in the crystal structure and its energy was compared with twice that of the single naphthalene molecules with the same geometry. As a result, the calculations with the M05-2X functional showed a preference for the dimeric naphthalene with a stabilization energy of 2.96 kcal mol^{-1}, whereas the B3LYP and M05

Table 3. Comparison of the experimental and calculated geometries of the C_2 isomers of compound **6**.

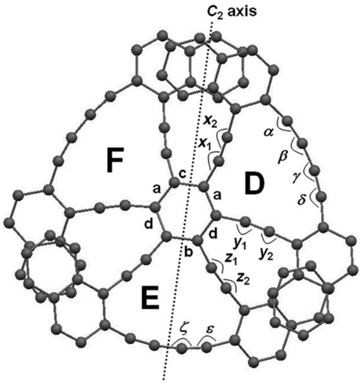

	X-ray	DFT/ B3LYP	DFT/M05	DFT/ M05-2X
endo bond length [Å]	$a = 1.424$	$a = 1.417$	$a = 1.413$	$a = 1.406$
	$b = 1.415$	$b = 1.419$	$b = 1.415$	$b = 1.408$
exo bond length [Å]	$c = 1.411$	$c = 1.446$	$c = 1.438$	$c = 1.430$
	d = 1.427	d = 1.442	d = 1.435	d = 1.428
core–blade dihedral angle [°][a]	30.73	36.52	31.19	28.94
"spoke" triple-bond angle [°]	$x_1 = 171.4$	$x_1 = 169.61$	$x_1 = 170.85$	$x_1 = 171.00$
	$x_2 = 172.7$	$x_2 = 175.94$	$x_2 = 174.68$	$x_2 = 174.39$
	$y_1 = 169.4$	$y_1 = 170.52$	$y_1 = 171.23$	$y_1 = 169.97$
	$y_2 = 175.0$	$y_2 = 176.05$	$y_2 = 173.86$	$y_2 = 172.70$
	$z_1 = 166.6$	$z_1 = 166.34$	$z_1 = 166.84$	$z_1 = 167.17$
	$z_2 = 176.6$	$z_2 = 176.85$	$z_2 = 175.84$	$z_2 = 175.02$
triple-bond angle in the diyne unit [°]	$\alpha = 168.7$	$\alpha = 166.94$	$\alpha = 168.26$	$\alpha = 168.72$
	$\beta = 167.8$	$\beta = 169.14$	$\beta = 168.47$	$\beta = 168.88$
	$\gamma = 168.7$	$\gamma = 168.45$	$\gamma = 168.48$	$\gamma = 169.47$
	$\delta = 165.0$	$\delta = 167.86$	$\delta = 168.43$	$\delta = 167.76$
	$\varepsilon = 170.6$	$\varepsilon = 169.13$	$\varepsilon = 169.67$	$\varepsilon = 169.33$
	$\zeta = 170.6$	$\zeta = 171.37$	$\zeta = 171.13$	$\zeta = 171.50$
dihedral angle between the naphthalene rings of the [14]DBA units [°][b]	1.78, 39.83	7.71, 34.86	6.85, 26.03	9.11, 22.46
dihedral angle between the peripheral naphthalene rings in adjacent [14]DBA units [°][c]	6.07, 37.44	29.91, 37.78	17.31, 19.87	13.18, 15.41

[a] Dihedral angles between the mean plane of the central benzene ring and that of the dinaphthylbutadiyne unit of ring E (24 carbon atoms in total; that is, C34–C57, Figure 2). [b] Dihedral angles between the mean planes of the two naphthalene units in rings E and D (i.e., C34–C43 versus C48–C57 and C4–C13 versus C18–C27, respectively, Figure 2). [c] Dihedral angles between the mean planes of the peripheral naphthalene rings in adjacent [14]DBA blades (i.e., C4–C13 versus C78–C87 and C18–C27 versus C34–C43, respectively, Figure 2).

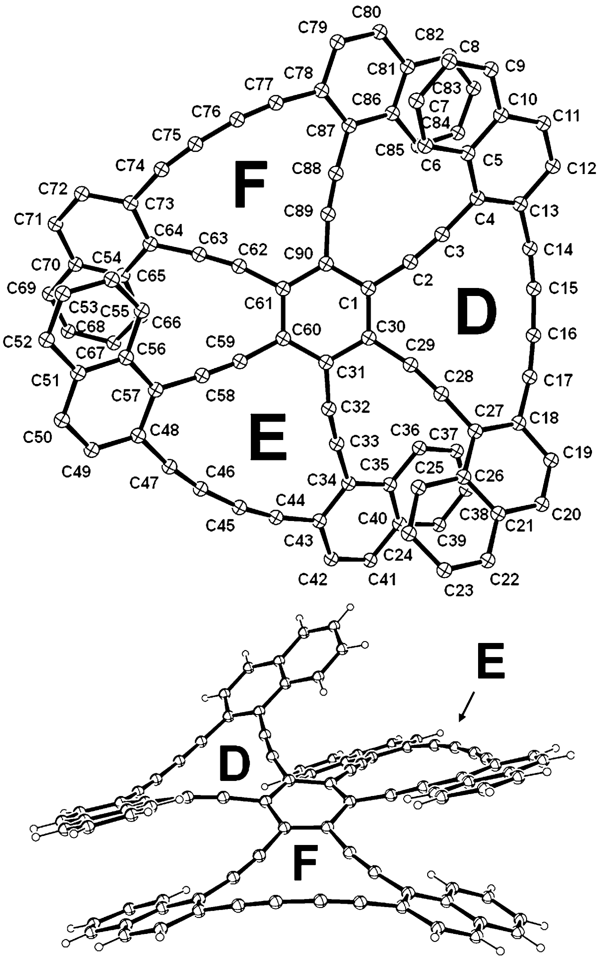

Figure 2. Molecular structure of compound **6** with atom-numbering, thermal ellipsoids at 30 % probability; solvent molecules are omitted for clarity (hydrogen atoms are omitted in the top structure for clarity).

methods exhibited repulsive interactions with destabilization energies of 4.72 and 0.12 kcal mol^{-1}, respectively. Therefore, we assume that the C_2 conformation of compound **6** is more stable than the D_3 isomer, mainly owing to π–π interactions between the naphthalene rings. Although these results conflict with Pascal's rule, in view of the large flexibility of the dehydro[14]annulene ring, it is reasonable to assume that the rule would no longer apply in molecular propellers that consist of [14]DBA units because the [14]annulene ring can be readily deformed from planarity without affecting the overlap of p orbitals in either the central- or peripheral aromatic rings. Either the C_2- or D_3 form will become favored, depending on subtle changes in the steric/electronic interactions.

Conformations- and dynamic behavior of compounds 4–6 in solution: X-ray crystallographic analysis showed that compounds **4** and **6** adopted D_3- and C_2-symmetric structures, respectively, in the crystalline state. Next, we investigated the conformations- and relevant dynamic behavior of compounds **4**–**6** in solution.

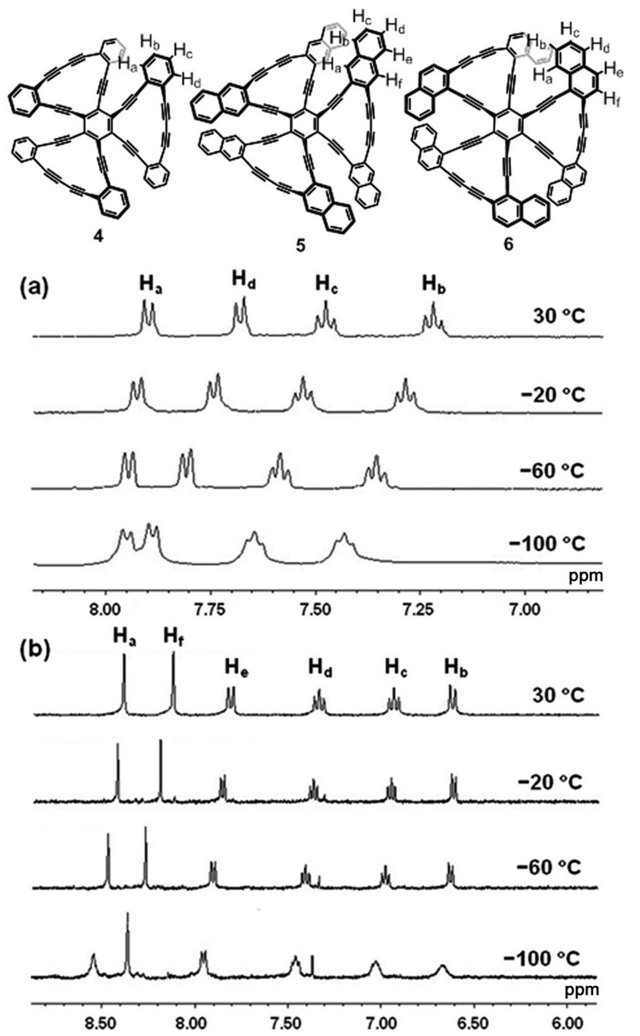

Figure 3. Region of the VT-^{1}H NMR spectra of a) compound **4** and b) compound **5** with assignment of the peaks (300 MHz, [D$_8$]THF, −100 to 30 °C).

The ^{1}H NMR spectra of compounds **4** and **5** at 30 °C (Figure 3 a, b) exhibited four- and six signals for the aromatic protons, respectively. Assignment of the signals was carried out on the basis of the coupling patterns and the calculated chemical shifts in the gas phase were derived from the GIAO-HF/6-31G* method for the D_3-conformers that were optimized by DFT calculations at the B3LYP/6-31G* level of theory (see the Supporting Information, Table S3).[24] We also performed the implicit solvent model of the ^{1}H NMR chemical-shift calculations[25] (for the methods and results of the solvent model, see the Supporting Information). The chemical shifts of compound **6** were also calculated for the C_2-conformer and were optimized by the M05-2X/6-31G* level of theory. The calculated chemical shifts by using the solvent model are in better agreement with the experimental results than those calculated for the gas phase. For compound **4**, although the observed- and calculated chemical shifts of the solvent model are in reasonable agreement ($\Delta\delta = < 0.1$ ppm), relatively large discrepancies ($\Delta\delta = 0.2$–

0.3 ppm) are observed for protons H_a and H_b (and H_c for compound **5**), which experience anisotropic effects of the aromatic ring of the adjacent [14]DBA unit. In the case of [14]DBA itself, the calculated chemical shifts agree better with those of the experimental shifts, although all of the calculated chemical shifts are uniformly downfield-shifted ($\Delta\delta = 0.15$–0.29 ppm by HF/6-31G* in the gas phase, $\Delta\delta = 0.05$–0.14 ppm by B3LYP/6-31G* in the solvent model calculation; see the Supporting Information, Figure S3).

The ^{13}C NMR spectrum of compound **4** at 30°C (see the Supporting Information, Figure S5) shows seven signals for the aromatic carbon atoms, whilst that of compound **5** shows eleven signals (see the Experimental Section), which is consistent with a D_3-symmetric conformation. However, the observation of highly-symmetric ^{1}H- and ^{13}C NMR signals indicates two possibilities regarding their conformational behavior in solution: 1) Both compounds **4** and **5** adopt D_3-symmetric structures and the ring-inversion into the C_2 form is too slow on the NMR timescale; or 2) the racemization takes place rapidly on the NMR timescale to exhibit time-averaged signals of the C_2- and D_3-symmetric conformations. In the former case, because the racemization of the D_3-conformers through the C_2 isomer should be slow, *P*- and *M* enantiomers of D_3-symmetric compounds **4** and **5** may be separated by chiral chromatography.[26] To this end, optical resolution by using a variety of chiral columns (see the Supporting Information) was attempted. However, despite intensive studies, the separation of the enantiomers of neither compound **4** nor **5** was observed, thus suggesting that the second possibility was more likely.

To gain an insight into the conformational equilibrium, we performed VT-NMR experiments. If the rate of ring-inversion becomes slow enough on the NMR timescale, line-broadening or the appearance of additional peaks owing to the less-symmetric C_2 conformation is expected. However, resolution of the ^{1}H NMR signals was not observed for both compounds **4** and **5**, even at −100°C (Figure 3), although apparent downfield shifts of some of the signals was observed.[27] On increasing the temperature, the ^{1}H NMR spectrum of compound **4** did not change (see the Supporting Information, Figure S4). Because the ^{13}C NMR measurements of compound **5** at low temperatures were hampered by low solubility, only low-temperature ^{13}C NMR measurements of compound **4** were performed. Whereas the spectrum at 30°C showed sharp, distinct signals, the signals at −100°C in [D$_8$]THF exhibited considerable broadening, thereby indicating a slowing of the exchange rate at this temperature. However, coalescence was not observed (see the Supporting Information, Figure S5).

Compound **4** crystallizes in the D_3 form, in agreement with the theoretical calculations, which predicted that the D_3 conformer was more stable than the C_2 form. However, the VT-NMR data did not provide any information regarding its conformation in solution and its dynamic behavior. Consequently, based on the theoretical calculations and the results of the chiral chromatography, we assume that compound **4** adopts the D_3 form, which racemizes rapidly through the C_2 isomers. Because compound **5** behaves like compound **4** in solution (with regard to the VT-NMR- and chiral-chromatography data), we assume that it also adopts the D_3 form with a low kinetic barrier for the C_2–D_3 or both the C_2–D_3 and C_2–C_2 interconversions.

In contrast to the VT-NMR spectra of compounds **4** and **5**, which did not give definitive information regarding their solution-state conformations, the ^{1}H NMR data of compound **6** provided an insight into its conformational behavior. First, the ^{1}H NMR spectrum at 150°C in [D$_4$]*p*-dichlorobenzene exhibited a sharp doublet signal for the naphthalene proton (H_a) at $\delta = 8.75$ ppm, which was resolved from the other aromatic proton signals (see the Supporting Information, Figure S6). As the temperature was lowered to 60°C, the signal became significantly broadened. In [D$_8$]toluene, a broad signal was also observed at 60°C, thereby indicating a slowing of the conformational exchange (Figure 4). Below 20°C, the signal was resolved into three doublets, which showed the presence of the C_2-symmetric conformation in solution and, at the same time, the absence of the D_3 conformer (as seen in the crystalline state). Notably, the decoalescence owing to the C_2-symmetric conformation is only observed when all of the interconversion rates become slow enough on the NMR timescale (see the Supporting Information, Scheme S6) because a time-averaged, highly-symmetric signal that corresponds to a mixture of interchanging conformations should be observed if only a part of the interconversion takes place rapidly. This behavior also suggests that the C_2–C_2 conversion rate becomes slow enough below 20°C on the NMR timescale and, more importantly, suggests the absence of the D_3 conformer of compound **6**, as indicated from the equal intensities of the three doublets. These results are consistent with those that were

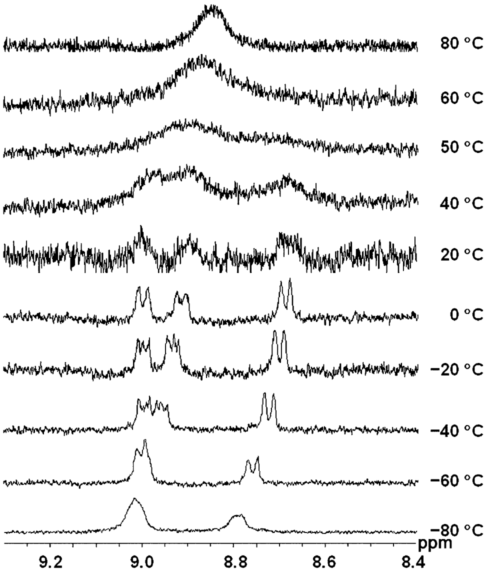

Figure 4. Region of the VT-^{1}H NMR spectra of compound **6** that shows the H_a proton (400 MHz, [D$_8$]toluene, −80 to 80°C).

based on the theoretical- and crystallographic studies (see above) in the sense that the C_2 conformer is more stable. The barrier for the C_2–C_2 interconversion was estimated to be 16.2 kcal mol^{-1} at the coalescence temperature (50 °C) of the two signals that were observed at lower fields ($\Delta\nu=33.2$ Hz). Upon further cooling to −80 °C, the two signals at lower fields started to recombine and the doublet at higher field became broadened again. This recombination of the signals can be attributed to an accidental isochrony of two different types of protons during the downfield shift on lowering the temperature.

Thus, compound **6** exhibited a conformational behavior that was different to that of hexabenzotriphenylene (**1**) but similar to that of hexamethyltriphenylene (**2**). In the former case, the D_3 isomer was estimated by a theoretical study to be more stable by about 8 kcal mol^{-1}.[3] The barrier for interconversion between the less-stable C_2 isomers was determined by VT-NMR spectroscopy to be 11.7 kcal mol^{-1} at 247 K, whereas that for the C_2–D_3 isomerization was determined by kinetic study of the C_2–D_3 conversion to be 26.2 kcal mol^{-1}.[4b] On the contrary, in the case of triphenylene derivative **2**, the barrier for the more-stable C_2–C_2 interconversion was determined by VT-NMR spectroscopy to be 10.2 kcal mol^{-1} at 220 K, whereas that for the C_2–D_3 isomerization was estimated by computational analysis to be about 25 kcal mol^{-1}.[2c] The barrier for the more-stable C_2–C_2 interconversion of compound **6** at 50 °C was estimated to be 16.2 kcal mol^{-1}. However, the barrier for the C_2–D_3 isomerization was not determined experimentally. This relatively low barrier, despite the large overlapping of the dehydroannulene blades, is ascribed to the flexibility of the acetylene linkages, which can be deformed substantially in the transition state of the ring flip.

Conclusions

In the solid state, molecular propeller **4**, which consists of [14]DBA blades, adopts an approximate D_3-symmetric structure, in which the individual [14]DBA ring twists substantially to avoid steric repulsion between the peripheral benzene rings. By contrast, naphthalene homologue **6** crystallizes in a C_2-symmetric structure, in which the acetylene units are strongly distorted such that two of the blades adopt an “arched” shape. The crystal structures were compared with those that were derived from the DFT calculations with different functionals. On the basis of the crystal structure and the relative energies that were estimated from the calculations with the M05-2X functional for the C_2- and D_3 conformers, together with the stabilization energy that was estimated for the naphthalene dimer model, we conclude that the C_2 conformer of compound **6** is stabilized by π–π interactions between the naphthalene units of a pair of adjacent blades. With regards to their dynamics in solution, VT-NMR experiments of compound **4** and **5** suggest that conformational interconversion take place rapidly on the NMR timescale, although no quantitative information was obtained. On the other hand, from the VT-NMR measurements of compound **6**, the barrier for the C_2–C_2 exchange was estimated to be 16.2 kcal mol^{-1}. Although these results are, at first, counterintuitive, in view of the overcrowded molecular structures, they are in accord with the remarkable flexibility of acetylene linkages in the rotational isomerism of sterically crowded acetylene derivatives.[13] These results are useful for the molecular design of shape-persistent- and shape-shifting[28] molecules that are based on [14]DBA or on other related dehydrobenzoannulene units, in particular when molecular flexibility and dynamic properties are in view.

Experimental Section

Compound 4: To a suspension of K_2CO_3 (132 mg, 0.955 mmol) in MeOH (20 mL) was added a solution of compound **9** (50.1 mg, 39.9 μmol) in THF (10 mL) under an argon atmosphere. After stirring for 10 h, the mixture was diluted with water and extracted with Et_2O. The extract was dried over anhydrous $MgSO_4$. Most of the solvent was removed under reduced pressure and the residue was dissolved in Et_2O (50 mL). This solution, which contained compound **10**, was added dropwise to a solution of $Cu(OAc)_2{\cdot}H_2O$ (398 mg, 1.99 mmol) in pyridine (100 mL) over a period of 9 h and the mixture was stirred for a further 3 h. The reaction was monitored by TLC and by laser-desorption-ionization (LDI) mass spectrometry. The reaction mixture was passed through a short column of silica gel ($CHCl_3$). After removal of the solvents, the products were separated by recycling gel-permeation chromatography (GPC) and recrystallized from $CHCl_3$/acetone to afford compound **5** (6.3 mg, 19 % yield)[16] as a pale-yellow solid, which decomposed gradually at RT.[29] ^{1}H NMR (300 MHz, [D$_8$]THF): $\delta=7.84$ (dd, $J=7.5$, 0.3 Hz, 6 H), 7.61 (dd, $J=7.5$, 1.5 Hz, 6 H), 7.38 (ddd, $J=7.5$, 7.5, 1.5 Hz, 6 H), 7.10 ppm (ddd, $J=7.5$, 7.5, 0.3 Hz, 6 H); ^{13}C NMR (75 MHz, [D$_8$]THF): $\delta=134.9$, 128.8, 128.6, 128.3, 127.3, 122.7, 101.1, 93.7, 86.7, 80.8 ppm; IR (KBr): $\tilde{\nu}=3058$, 2924, 2851, 2214, 2168, 1507, 1470, 1448, 1385, 754, 667, 580 cm^{-1}; MS (FAB): m/z: 816 $[M]^+$.

Compound 5: To a suspension of K_2CO_3 (110 mg, 0.796 mmol) in MeOH (40 mL) was added a solution of compound **14** (82.9 mg, 53.3 μmol) in THF (15 mL) under an argon atmosphere. After stirring for 3 h, the mixture was diluted with water and extracted with CH_2Cl_2 (20 mL). The extract was diluted with THF (80 mL). This solution, which contained compound **15**, was added dropwise to a solution of $Cu(OAc)_2{\cdot}H_2O$ (570 mg, 2.85 mmol) in a degassed (by bubbling with argon for 15 min) mixture of pyridine (80 mL) and CH_3CN (20 mL) over a period of 12 h. The mixture was stirred for 12 h at RT before and then passed through a short column of silica gel ($CHCl_3$). After removal of the solvent, the residue was washed with CH_3CN. The residual solid was purified by recycling GPC and HPLC (ODS column, CH_2Cl_2/CH_3CN, 7:13) to afford compound **5** as a pale-yellow solid, which decomposed rapidly at RT.[29] ^{1}H NMR (300 MHz, [D$_8$]THF): $\delta=8.39$ (s, 6 H), 8.12 (s, 6 H), 7.83 (d, $J=8.1$ Hz, 6 H), 7.34 (dd, $J=8.1$, 7.8 Hz, 6 H), 6.94 (dd, $J=8.1$, 7.8 Hz, 6 H), 6.63 ppm (d, $J=8.1$ Hz, 6 H); ^{13}C NMR (75 MHz, [D$_8$]THF): $\delta=136.6$, 133.31, 133.25, 130.0, 129.2, 128.7, 128.4, 128.3, 128.2, 124.9, 120.1, 102.0, 93.4, 87.8, 81.3 ppm; MS (LDI, negative mode): m/z: 1116.9 $[M]^-$.

Compound 6: To a suspension of K_2CO_3 (134 mg, 0.970 mmol) in MeOH (30 mL) was added a solution of compound **17** (99.7 mg, 64.1 μmol) in THF (50 mL). After stirring at RT for 3.5 h under an argon atmosphere, an aqueous solution of NH_4Cl was added and the reaction mixture was extracted with Et_2O. The extract was washed with brine and diluted with Et_2O (80 mL). This solution, which contained compound **18**, was added dropwise to a solution of $Cu(OAc)_2{\cdot}H_2O$ (1.28 g, 6.41 mmol) in a degassed (by bubbling with argon for 15 min) mixture of pyridine (100 mL) and CH_3CN (20 mL) over a period of 18 h at 70 °C. The mixture was stirred for a further 2 h at 70 °C before it was passed through a short column of silica gel ($CHCl_3$). After removal of the solvent, the residue was purified by recycling GPC to afford compound **6** (5.1 mg, 7%) as an orange solid, which decomposed gradually at RT.[29,30] ^{1}H NMR (400 MHz, [D$_4$]*p*-dichlorobenzene, 150°C): $\delta = 8.74$ (d, $J = 8.0$ Hz, 6H), 7.35 (d, $J = 8.4$ Hz, 6H), 7.29 (d, $J = 8.4$ Hz, 6H), 7.12 (d, $J = 8.0$ Hz, 6H), 6.84 (dd, $J = 7.6$, 6.8 Hz, 6H), 6.79 ppm (dd, $J = 7.6$, 6.8 Hz, 6H); MS (LDI, negative mode): m/z: 1116.7 $[M]^-$.

Crystal data: CCDC-872771 (**4**) and CCDC-872772 (**6**) contain the supplementary crystallographic data for this paper. These data can be obtained free of charge from The Cambridge Crystallographic Data Centre via www.ccdc.cam.ac.uk/data_request/cif.

Acknowledgements

This work was supported by a Grant-in-Aid for Scientific Research from the Ministry of Education, Culture, Sports, and Technology, Japan. The authors thank Professor Yoshio Okamoto (Nagoya University) for the chiral chromatography experiments, Professors Shinji Toyota (Okayama University of Science) and Gaku Yamamoto (Kitasato University) for their valuable suggestions regarding dynamic NMR spectroscopy, and Dr. Ichiro Hisaki (Osaka University) for his help with the X-ray crystallographic analysis.

---

[1] For a review on overcrowded polycyclic aromatic compounds, see: R. A. Pascal, Jr., *Chem. Rev.* **2006**, *106*, 4809–4819.

[2] a) M. B. Hursthouse, V. B. Smith, *J. Fluorine Chem.* **1977**, *10*, 145–155; b) C. S. Frampton, D. D. MacNicol, S. J. Rowan, *J. Mol. Struct.* **1997**, *405*, 169–178; c) Y. Wang, A. D. Stretton, M. C. McConnell, P. A. Wood, S. Parsons, J. B. Henry, A. R. Mount, T. H. Galow, *J. Am. Chem. Soc.* **2007**, *129*, 13193–13200.

[3] L. Barnett, D. M. Ho, K. K. Baldridge, R. A. Pascal, Jr., *J. Am. Chem. Soc.* **1999**, *121*, 727–733.

[4] a) D. Peña, D. Pérez, E. Guitián, L. Castedo, *Org. Lett.* **1999**, *1*, 1555–1557; b) D. Peña, A. Cobas, D. Pérez, E. Guitián, L. Castedo, *Org. Lett.* **2000**, *2*, 1629–1632.

[5] M. A. Bennett, M. R. Kopp, E. Wenger, A. C. Willis, *J. Organomet. Chem.* **2003**, *667*, 8–15.

[6] C. Romero, D. Peña, D. Pérez, E. Guitián, *Chem. Eur. J.* **2006**, *12*, 5677–5684.

[7] J. M. Alonso, A. E. Díaz-Álvarez, A. Criado, D. Pérez, D. Peña, E. Guitián, *Angew. Chem.* **2012**, *124*, 177–181; *Angew. Chem. Int. Ed.* **2012**, *51*, 173–177.

[8] a) K. Zimmermann, R. Goddard, C. Krüger, M. W. Haenal, *Tetrahedron Lett.* **1996**, *37*, 8371–8374; b) J. K. Gimzewski, C. Joachim, P. R. Schlittler, V. Langlais, H. Tang, I. Johannsen, *Science* **1998**, *281*, 531–533; c) B. Iglesias, D. Peña, D. Pérez, E. Guitián, L. Castedo, *Synlett* **2002**, 0486–0488.

[9] A. Pradhan, P. Dechambenoit, H. Bock, F. Durola, *Angew. Chem.* **2011**, *123*, 12790–12793; *Angew. Chem. Int. Ed.* **2011**, *50*, 12582–12585.

[10] T. Yoshimura, A. Inaba, M. Sonoda, K. Tahara, Y. Tobe, R. V. Williams, *Org. Lett.* **2006**, *8*, 2933–2936.

[11] K. Tahara, T. Yoshimura, M. Sonoda, Y. Tobe, R. V. Williams, *J. Org. Chem.* **2007**, *72*, 1437–1442.

[12] For previous syntheses of [14]DBA and its derivatives, see: a) K. P. Baldwin, A. J. Matzger, D. A. Scheiman, C. A. Tessier, K. P. C. Vollhardt, W. J. Youngs, *Synlett* **1995**, 1216–1218; b) J. A. Marsden, J. J. Miller, M. M. Haley, *Angew. Chem.* **2004**, *116*, 1726–1729; *Angew. Chem. Int. Ed.* **2004**, *43*, 1694–1697.

[13] a) S. Toyota, T. Yamamori, T. Makino, *Tetrahedron* **2001**, *57*, 3521–3528; b) T. Makino, S. Toyota, *Bull. Chem. Soc. Jpn.* **2005**, *78*, 917–928; c) S. Toyota, *Chem. Rev.* **2010**, *110*, 5398–5424.

[14] Recently, Haley and co-workers reported the synthesis- and optical properties of trefoil-shaped molecules in which three [14]DBA rings were fused to a central triphenylene, -dehydrobenzo[12]annulene, or -dehydrobenzo[18]annulene core. However, because of the large core size, these compounds would not exhibit hindered rotation around the [14]DBA blades. See: T. Takeda, A. G. Fix, M. M. Haley, *Org. Lett.* **2010**, *12*, 3824–3827.

[15] a) C. Huynh, G. Linstrumelle, *Tetrahedron* **1988**, *44*, 6337–6344; b) J. A. John, J. M. Tour, *J. Am. Chem. Soc.* **1994**, *116*, 5011–5012.

[16] About one-sixth of the volume of an eluent from GPC analysis that contained purified compound **4** was evaporated to dryness, the residue was weighed, and its purity was checked by NMR spectroscopy. From this experiment, the yield of compound **4** was estimated to be approximately 24% by using $CHBr_3$ as an internal standard.

[17] a) R. Diercks, J. C. Armstrong, R. Boese, K. P. C. Vollhardt, *Angew. Chem.* **1986**, *98*, 270–271; *Angew. Chem. Int. Ed. Engl.* **1986**, *25*, 268–269; b) T. X. Neenan, G. M. Whitesides, *J. Org. Chem.* **1988**, *53*, 2489–2496; c) M. Sonoda, A. Inaba, K. Itahashi, Y. Tobe, *Org. Lett.* **2001**, *3*, 2419–2421.

[18] Several hexaethynylbenzene derivatives have been prepared by substitution with compound **12**, see: a) S. Ito, H. Inabe, N. Morita, K. Ohta, T. Kitamura, K. Imafuku, *J. Am. Chem. Soc.* **2003**, *125*, 1669–1680; b) J. Nierle, D. Barth, D. Kuck, *Eur. J. Org. Chem.* **2004**, 867–872; c) M. Hasegawa, H. Enozawa, Y. Kawabata, M. Iyoda, *J. Am. Chem. Soc.* **2007**, *129*, 3072–3073; d) M. Schmittel, P. Mal, *Chem. Commun.* **2008**, 960–962.

[19] a) Y. Zhao, N. E. Schultz, D. G. Truhlar, *J. Chem. Phys.* **2005**, *123*, 161103; b) Y. Zhao, N. E. Schultz, D. G. Truhlar, *J. Chem. Theory Comput.* **2006**, *2*, 364–382; c) Y. Zhao, D. G. Truhar, *J. Chem. Theory Comput.* **2006**, *2*, 1009–1018; d) S. Toyota, H. Miyahara, M. Goichi, S. Yamasaki, T. Iwanaga, *Bull. Chem. Soc. Jpn.* **2009**, *82*, 931–945.

[20] For a [14]DBA ring, "spoke" bond angles of 168–172° have been reported; see: a) K. P. Baldwin, A. J. Matzger, D. A. Scheiman, C. A. Tessier, K. P. C. Vollhardt, W. J. Youngs, *Synlett* **1995**, 1215–1218; b) H. Hinrichs, A. K. Fischer, P. G. Jones, H. Hopf, M. M. Haley, *Org. Lett.* **2005**, *7*, 3793–3795; c) H. S. Blanchette, S. C. Brand, H. Naruse, T. J. R. Weakley, M. M. Haley, *Tetrahedron* **2000**, *56*, 9581–9588; d) M. J. O'Connor, R. B. Yelle, L. N. Zakharov, M. M. Haley, *J. Org. Chem.* **2008**, *73*, 4424–4432.

[21] a) W. B. Wan, M. M. Haley, *J. Org. Chem.* **2001**, *66*, 3893–3901; b) K. West, C. Wang, A. S. Batsanov, M. R. Bryce, *J. Org. Chem.* **2006**, *71*, 8541–8544.

[22] a) Q. Zhou, P. J. Carroll, T. M. Swager, *J. Org. Chem.* **1994**, *59*, 1294–1301; b) I. Hisaki, T. Eda, M. Sonoda, H. Niino, T. Sato, T. Wakabayashi, Y. Tobe, *J. Org. Chem.* **2005**, *70*, 1853–1864.

[23] Another dihedral angle between the mean planes of two almost-planar butadiyne-bridged naphthalene rings in ring E (i.e., C34–C43 versus C48–C57) was 1.8°.

[24] For the chemical-shift calculations we used the HF method because this had been shown to be the most reliable means for evaluating the chemical shifts (i.e., magnetic properties) of annulenes. For example, see: R. V. Williams, J. R. Armantrout, B. Twamley, R. H. Mitchell, T. R. Ward, S. Bandyopadhyay, *J. Am. Chem. Soc.* **2002**, *124*, 13495–13505.

[25] a) R. Jain, T. Bally, P. R. Rablen, *J. Org. Chem.* **2009**, *74*, 4017–4023; b) T. Bally, P. R. Rablen, *J. Org. Chem.* **2011**, *76*, 4818–4830; c) M. Cossi, G. Scalmani, N. Rega, V. Barone, *J. Chem. Phys.* **2002**, *117*, 43–54.

[26] a) Y. Okamoto, T. Ikai, *Chem. Soc. Rev.* **2008**, *37*, 2593–2608; b) T. Ikai, Y. Okamoto, *Chem. Rev.* **2009**, *109*, 6077–6101.

[27] The latter behavior can be attributed to the change in the ratio of the conformational population. As shown in the Supporting Information, Table S3, for both compounds **4** and **5**, the calculated chemical shifts of the D_3 structure are shifted downfield compared to those of the C_2 structure. Hence, upon lowering the temperature, the observed downfield shifts are presumably due to the population of the more-stable D_3 conformers.

[28] a) A. R. Lippert, A. Naganawa, V. L. Keleshian, J. W. Bode, *J. Am. Chem. Soc.* **2010**, *132*, 15790–15799; b) M. He, J. W. Bode, *Proc. Natl. Acad. Sci. USA* **2011**, *108*, 14752–14756.

[29] Because of the instability of the material, the melting point was not determined.

[30] Compound **6** was barely soluble in any solvent and was only slightly soluble in aromatic solvents, such as toluene and *p*-dichlorobenzene, at elevated temperature. The ^{13}C NMR spectrum of compound **6** is not reported because the intensities of the signal were low and most of the signals overlapped with the signals of the aromatic solvent and, hence, were concealed by them.

Received: March 29, 2012
Revised: June 10, 2012

Annulenes

*S. Nobusue, Y. Mukai, Y. Fukumoto,
R. Umeda, K. Tahara, M. Sonoda,
Y. Tobe** .... ▮▮▮▮–▮▮▮▮

Molecular Propellers that Consist of Dehydrobenzo[14]annulene Blades

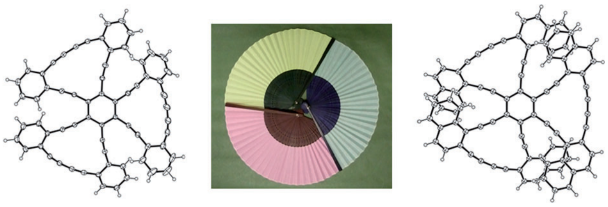

The propellerheads: The behavior of propeller-shaped compounds with dehydrobenzo[14]annulene rings was investigated. Interconversion between the stereoisomers had relatively small energy barriers owing to the flexibility of the acetylene linkages.